

# EXISTENCE OF STABLE PERIODIC ORBITS IN BILLIARDS CLOSE TO LEMON AND MOON BILLIARDS

ALEXANDER GRIGO

ABSTRACT. It is known that at lemon and moon billiards that have a sufficiently small curvature on one of their circular arcs are hyperbolic. In this paper we show that replacing this circular arc by a more general boundary component of small curvature could produce billiard tables that admit nonlinearly stable periodic orbits.

## CONTENTS

1. Introduction and main results	1
2. Construction of special periodic orbits	5
3. Stability of the periodic orbit	7
4. Examples of boundary components with elliptic periodic orbits	10
4.1. Boundary components with positive curvature	10
4.2. Strictly convex boundary components	11
References	14

## 1. INTRODUCTION AND MAIN RESULTS

The billiard flow describes the motion of a point particle along straight lines inside a domain (billiard table) with specular reflections off the boundary components. The associated billiard map is the map induced by the billiard flow going from one reflection off the boundary to the next. The mathematical tools to investigate dynamical properties of billiards are best developed for billiards in two-dimensional domains.

The first rigorous proof of hyperbolicity and ergodicity of some billiards was carried out by Sinai in [17]. The billiard domains he considered are now called dispersing or Sinai billiards, which consist of boundary components with strictly positive curvature only. One such billiard table is shown in Fig. 1. Hyperbolicity in dispersing billiards is due to the fact that dispersing fronts of billiard trajectories remain dispersing and expand exponentially from collision to collision in a geometrically intuitive way.

Because of the clear geometric mechanism for hyperbolicity in dispersing billiards it came as a surprise that just a few years after Sinai's work Bunimovich proved in [2–4] hyperbolicity and ergodicity of billiard tables with focusing boundary components. In fact, some of the billiard tables he considered were convex. An example of such a Bunimovich billiard is shown in Fig. 1. Hyperbolicity in Bunimovich billiards is due to the so-called defocusing mechanism, which requires that if fronts of billiard trajectories become focusing due to a reflection off a focusing

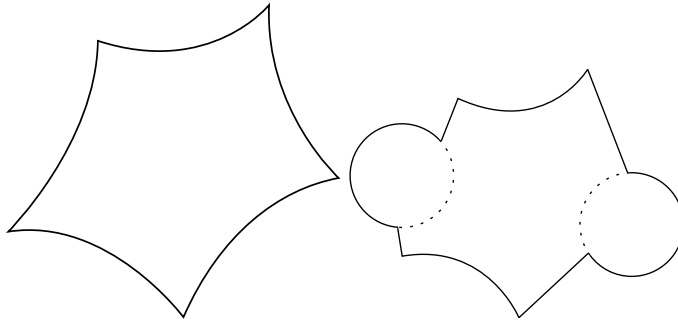


FIGURE 1. Examples of Sinai billiards (left) and Bunimovich billiards (right).

boundary component, then the free path after the last reflection off that boundary component must be long enough to ensure that the front of billiard trajectories will become dispersing and expands sufficiently before the next collision off a boundary component. A convenient way to implement this mechanism is to allow only arcs of circles for focusing boundary components. In this case the defocusing mechanism is guaranteed by an easy to verify geometric condition: for each circular arc the entire circle is contained inside the billiard table. This is indicated by the dashed lines in Fig. 1.

For a detailed exposition of dispersing billiards and an introduction to Bunimovich billiards we refer the reader to [12]. For hyperbolic billiards with more general types of focusing boundary components we refer the reader to [5–8, 14, 16, 18].

A particular Bunimovich billiard that will be considered in this paper is a particular version of what is sometimes called flower billiard, namely a flower billiard with two petals. This billiard table consists of the union of two overlapping circles. In the special case that these two circles have the same radius, as is shown in Fig. 2, the resulting table has a reflection symmetry about the dashed line shown in Fig. 2.

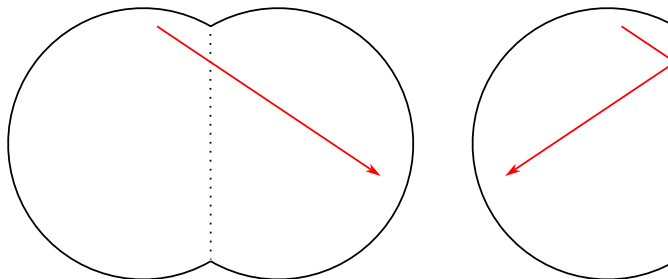


FIGURE 2. Symmetric flower billiard with two petals and the corresponding folded flower table.

Cutting the symmetric two petal flower billiard table along that axis (and removing the right half) and inserting a straight line boundary component we obtain a reduced or folded billiard table, shown in the right side of Fig. 2. The billiard dynamics in the folded table is essentially equivalent to the billiard dynamics of the two petal flower billiard table. This orbit equivalence is indicated in Fig. 2 by displaying two related billiard trajectory segments.

There are two modifications of the folded flower table that have been considered in the literature. One is obtained by replacing the straight line segment by a circular arc that becomes a focusing boundary component and thus results in a convex table. These billiards are sometimes called lemon billiards. The other is obtained by replacing the straight line by a circular arc that becomes a dispersing boundary component. These billiards are sometimes called moon billiards. Both of these are illustrated in Fig. 3.

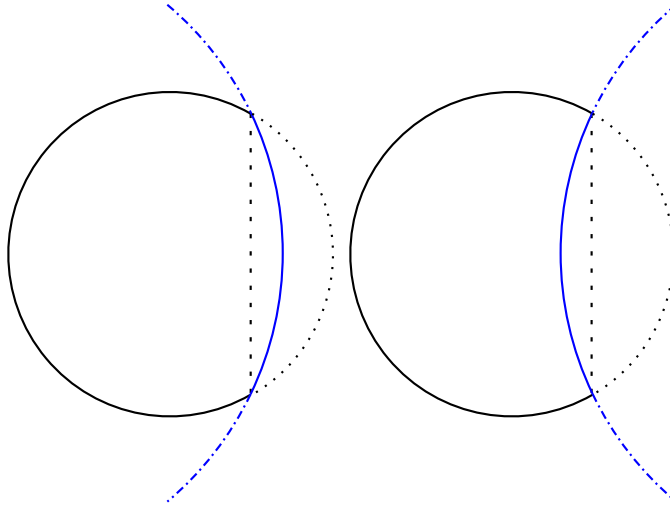


FIGURE 3. Modifications of the folded flower billiard to a lemon billiard and to a moon billiard.

It is important to note that neither the lemon billiard nor the moon billiard is a Bunimovich billiard, and that the defocusing mechanism fails for both of them. Therefore, hyperbolicity of either table is not immediately implied by classic results available in the literature, nor is there a clear mechanism for hyperbolicity readily available.

If the curvature of the added circular arc is very small we may think of the resulting lemon or moon billiard as a small perturbation of the folded flower billiard. And since the folded flower billiard is hyperbolic, as shown by Bunimovich's work, it might seem reasonable to expect that perturbations of the folded flower billiard to either a lemon or moon billiard are also hyperbolic.

Indeed, the hyperbolicity of such lemon billiards was first investigated in [10] and later rigorously proven in [15]. Numerical evidence for the hyperbolicity of such moon billiards was established in [13]. For large curvatures of the added circular arc the resulting moon billiards can exhibit elliptic periodic orbits as was shown in [13]. (See also [1] for related work on annular billiards.)

In the present paper we consider other modifications of the folded flower billiard by replacing the straight line segment not by arcs of a circle, but by a more general boundary component. An illustration of such a  $\Gamma$  is shown in Fig. 4. If the curvature of  $\Gamma$  is uniformly small the resulting billiard table is a small geometric perturbation of the folded flower table, just as the lemon and moon tables were. Again one might expect that the resulting billiard will be hyperbolic. However, in the present paper it will be shown that this is not always so.

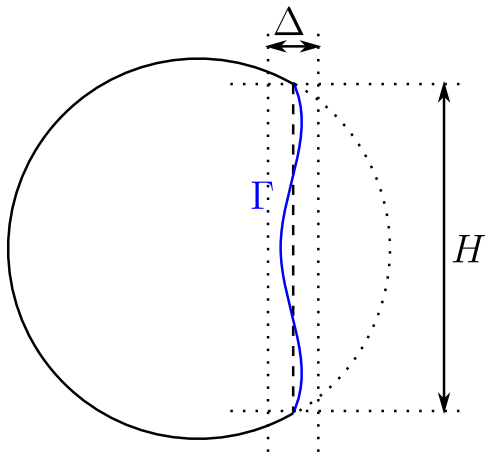


FIGURE 4. Perturbations of the folded two-petal flower billiard.

In order to state a precise version of this we need to introduce some notation. Let  $H > 0$  denote the height of the straight line segment in the folded flower table. Let  $\Delta > 0$  denote the width of a vertical strip containing the vertical line segment. Note that for the circular arcs used to construct the perturbation to a lemon or a moon billiard the corresponding curvature (in absolute value) multiplied by  $H$  is of the same order as the horizontal width it occupies inside the resulting table divided by  $H$ . Therefore, we will consider boundary components  $\Gamma$  whose curvature  $\mathcal{K}$  (in absolute value) multiplied by  $H$  is of the same order as  $\frac{\Delta}{H}$ . And  $\Delta$  is taken to be arbitrarily small.

**Theorem 1.1.** *There exists a countably infinite set  $S$  such that for each  $H \in S$  the following hold.*

- (1) *There exists a constant  $C > 0$  so that for all  $\Delta > 0$  small enough there exists a piece-wise smooth  $\Gamma$  that is entirely contained in the vertical strip of width  $\Delta$ , with  $|\mathcal{K}|H \leq C \frac{\Delta}{H}$  on  $\Gamma$ , and such that the resulting perturbed billiard table admits a nonlinearly stable periodic orbit  $\gamma$  with non-vanishing first Birkhoff coefficient.*
- (2)  *$\Gamma$  can be taken to be symmetric about the horizontal symmetry axis (see Fig. 4), and to also satisfy one of the following properties*
  - (a)  *$\Gamma$  is everywhere smooth and  $\mathcal{K} > 0$  at all points where  $\gamma$  reflects off  $\Gamma$ .*
  - (b)  *$\Gamma$  is piece-wise smooth and  $\mathcal{K} > 0$  on  $\Gamma$ .*
  - (c)  *$\Gamma$  is everywhere smooth, strictly convex with  $\mathcal{K} < 0$  everywhere on  $\Gamma$ .*

The existence of  $\Gamma$  with all its properties claimed in Theorem 1.1 is stable under small  $C^5$  perturbations of  $\Gamma$ , so that we obtain an open set (in the  $C^5$  topology) of billiard tables that contains arbitrarily small (in the sense of curvature) perturbations of the folded flower table which admit nonlinearly stable periodic orbits.

The remainder of the paper establishes a proof of Theorem 1.1. In Section 2 we describe the general part of our construction of  $\Gamma$  and the choice of the special values of  $H$  given by  $S$  in Theorem 1 that give rise to a special periodic orbit  $\gamma$ . In Section 3 we derive a criterion for the stability of the periodic orbit  $\gamma$ . Both together will provide a proof for Item (1) of Theorem 1.1. It will become clear that

the construction used does not depend on any symmetry assumptions and is able to produce asymmetric boundary components  $\Gamma$  for which the resulting billiard table admits stable periodic orbits that are not symmetric either. For simplicity, however, we shall only consider the more restrictive case of symmetric  $\Gamma$  in detail.

The final Section 4 provides examples of boundary components that satisfy additional properties, and thus completes the proof of Theorem 1.1. That section is split into two parts.

In the first part, Section 4.1, we describe constructions of smooth  $\Gamma$  such that the stable periodic orbit  $\gamma$  reflects off  $\Gamma$  only in places where the curvature is strictly positive. As will become clear, our construction will require  $\Gamma$  to also have parts with negative curvature to retain the smoothness of  $\Gamma$ . If only a piece-wise smooth  $\Gamma$  is required, then we will construct examples of such  $\Gamma$  that have positive curvature only. This latter result is in stark contrast with the hyperbolicity of perturbations to moon billiards as established numerically in [13].

The second part, found in Section 4.2, describes the construction of smooth components  $\Gamma$  that are strictly convex. This result is in stark contrast with the hyperbolicity of perturbations of the folded flower billiard to lemon billiards established in [10, 15].

## 2. CONSTRUCTION OF SPECIAL PERIODIC ORBITS

Fix a circle of radius  $r$  and an integer  $N \geq 3$ , and consider an  $N$ -periodic orbit inside the circle with one of its segments oriented so that it is vertical, as indicated by the dotted polygon in Fig. 5 for  $N = 5$ . This vertical segment is where the place

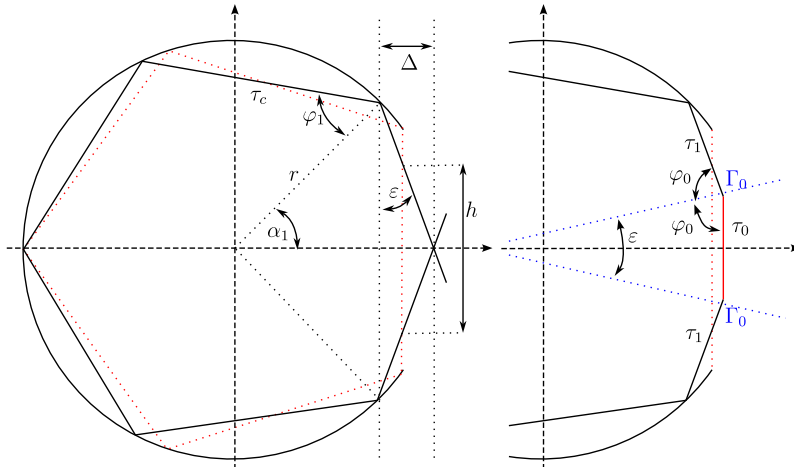


FIGURE 5. Construction of a billiard orbit segment (left figure) that will be used to produce an elliptic periodic orbit of period  $N + 2$  (right figure).

the cut to make the circle into a folded flower billiard table. In particular

$$(1) \quad H = 2r \sin \frac{\pi}{N}$$

is the value of  $H$  for that folded flower table. The collection of all such values of  $H$  indexed by  $N \geq 3$  provides the countably infinite set  $S$  claimed in Theorem 1.1.

Increasing the angle of reflection while keeping the symmetry about the horizontal axis results in a billiard orbit segment having  $N$  reflections off the circle as shown in Fig. 5. In particular, the initially vertical orbit segment is broken up and is no longer vertical. The resulting angle with the vertical axis will be denoted by  $\varepsilon$ . Note that  $\varepsilon > 0$ . Due to the symmetry the two orbit segments that resulted from breaking up the initially vertical segment intersect exactly on the horizontal symmetry axis. The horizontal distance between that intersection point and the first point of reflection on the circular arc will be denoted by  $\Delta$ . Those two orbit segments also intersect the initially vertical segment. The distance between these two intersection points will be denoted by  $h$ . Furthermore, the polar angle corresponding to the first reflection off the circular arc is denoted by  $\alpha_1$ , and the corresponding angle of reflection is denoted by  $\varphi_1$ .

The symmetry about the horizontal axis then requires that  $\varepsilon$ ,  $\varphi_1$  and  $\alpha_1$  are related by  $2\alpha_1 + (N-1)(\pi - 2\varphi_1) = 2\pi$  and  $\alpha_1 + \varphi_1 + \frac{\pi}{2} - \varepsilon = \pi$ , i.e.  $\alpha_1 = \frac{\pi}{2} - \varphi_1 + \varepsilon$ . Therefore we can use  $\varepsilon$  to express  $\alpha_1$  and  $\varphi_1$  as follows:

$$(2) \quad \alpha_1 = \frac{\pi}{N} + \frac{N-1}{N} \varepsilon, \quad \frac{\pi}{2} - \varphi_1 = \frac{\pi}{N} - \frac{1}{N} \varepsilon.$$

For the length  $\tau_c$  of the free path along the circular arc we have  $\tau_c = 2r \cos \varphi_1$ , and hence

$$(3) \quad \tau_c = 2r \sin \left( \frac{\pi}{N} - \frac{1}{N} \varepsilon \right) = 2r \sin \frac{\pi}{N} + \mathcal{O}(\varepsilon)$$

follows. The expressions for  $\Delta$

$$(4) \quad \Delta = r \sin \alpha_1 \tan \varepsilon$$

and  $h$

$$(5) \quad h = 2r \sin \alpha_1 - 2r \frac{\cos \frac{\pi}{N} - \cos \alpha_1}{\tan \varepsilon} = \frac{1}{N} \tau_c + \mathcal{O}(\varepsilon) = \frac{1}{N} 2r \sin \frac{\pi}{N} + \mathcal{O}(\varepsilon)$$

are both readily obtained from Fig. 5.

In order to generate a periodic orbit  $\gamma$  we add a new boundary component  $\Gamma$  such that the two orbit segments that broke off the initially vertical segment intersect  $\Gamma$ . We may as well make  $\Gamma$  symmetric about the horizontal symmetry axis. Denote the two points of intersection by  $\Gamma_0$  (they are symmetric about the horizontal axis, so we use the same symbol to denote both) as shown in Fig. 5. Furthermore, we make the tangent line at  $\Gamma_0$  such that the orbit segments will reflect off  $\Gamma_0$  at an angle  $\varphi_0$  that will produce a vertical outgoing orbit segment. Thus we obtain a periodic orbit  $\gamma$  of period  $N + 2$ , provided that  $\Gamma$  is also chosen to not introduce any additional intersection (would-be reflections) with  $\gamma$ .

We denote the free path from  $\Gamma_0$  to the circular arc by  $\tau_1$ , and we use  $\tau_0$  to denote the free path between  $\Gamma_0$  and its symmetric copy, which corresponds to the length of the vertical orbit segment of  $\gamma$  connecting  $\Gamma_0$  and its symmetric copy.

It is evident from this construction of the  $N + 2$  periodic orbit, see also the illustration shown in Fig. 5, that  $\varphi_1 + \varphi_0 + \alpha_1 - \frac{1}{2}\varepsilon = \pi$ . Thus, using (2) it follows that

$$(6) \quad \frac{\pi}{2} - \varphi_0 = \frac{1}{2}\varepsilon$$

as indicated in Fig. 5.

There is, however, a relation between  $\tau_0$ ,  $\tau_1$  and the value of  $\varepsilon$ . Clearly, given  $\varepsilon$  the value of  $\tau_0$  can be anywhere in the range:

$$(7) \quad 0 < \tau_0 < 2r \sin \alpha_1$$

And for any such choice of  $\tau_0$  we then have fixed the location of  $\Gamma_0$ . The corresponding normal line must always have angle  $\frac{\varepsilon}{2}$  with the horizontal axis. The value of  $\tau_1$  is then also fixed, and must satisfy the relation

$$r \sin \alpha_1 - \frac{1}{2}\tau_0 = \tau_1 \cos \varepsilon$$

as can be readily seen from Fig. 5. Therefore, we have

$$(8) \quad \tau_1 = \frac{2r \sin \alpha_1 - \tau_0}{2 \cos \varepsilon}$$

for  $\tau_1$  as a function of  $\varepsilon$  and  $\tau_0$ .

To summarize the above construction, fix any  $N \geq 3$  and any (small) value of  $\varepsilon > 0$ . For any choice of  $\tau_0$  in the admissible range (7) there exists an  $N + 2$  periodic orbit  $\gamma$ , that can be chosen to be symmetric about the horizontal axis, as shown in Fig. 5. Notice that only the location of  $\Gamma_0$  (fixed by the choice of  $\tau_0$ ), and the corresponding normal line (whose angle with the horizontal axis is  $\frac{\varepsilon}{2}$ ) are fixed by the above construction. The local (and global) geometry of the boundary component  $\Gamma$  near  $\Gamma_0$  does not affect the periodic orbit  $\gamma$ , as long as  $\Gamma$  does not have other intersections with  $\gamma$  (which would prevent  $\gamma$  from existing as described in the above construction).

This establishes the countably infinite set  $S$  in Theorem 1.1, and the existence  $\Gamma$  that gives rise to a periodic orbit  $\gamma$ . The corresponding stability claim of Item (1) in Theorem 1.1 will be addressed in the next section.

### 3. STABILITY OF THE PERIODIC ORBIT

Fix  $r$ ,  $N$ ,  $\varepsilon$ ,  $\tau_0$  and consider the periodic orbit  $\gamma$  as constructed in Section 2. Recall that the construction of  $\gamma$  described above does not determine the boundary component  $\Gamma$  globally. Only conditions on the local geometry of any such  $\Gamma$  are specified. Let  $\mathcal{K}_0$  denote the curvature of (any one such)  $\Gamma$  at  $\Gamma_0$ . While the global description of  $\Gamma$  is essential in order to prove existence of  $\gamma$  as described in Section 2, it is only the local geometry that matters for the stability analysis of  $\gamma$ . This will be carried out in this section, while we postpone the global description of  $\Gamma$  until the next section.

The linearization of the billiard flow, see [12] for details, from right before the first reflection off the circular arc to right after the  $N$ -th reflection off the circular arc will be denoted by  $L_c$  and is given by

$$L_c = \left[ \begin{pmatrix} -1 & 0 \\ \frac{4}{\tau_c} & -1 \end{pmatrix} \begin{pmatrix} 1 & \tau_c \\ 0 & 1 \end{pmatrix} \right]^N \begin{pmatrix} -1 & 0 \\ \frac{4}{\tau_c} & -1 \end{pmatrix}.$$

It is not difficult to establish that

$$(9) \quad L_c = \begin{pmatrix} 1 - 2N & (N - 1)\tau_c \\ \frac{4N}{\tau_c} & 1 - 2N \end{pmatrix}$$

holds.

Therefore, the linearization of the billiard flow around the entire periodic orbit  $\gamma$ , which will be denoted by  $M$ , is given by

$$(10) \quad M = L_c \begin{pmatrix} 1 & \tau_1 \\ 0 & 1 \end{pmatrix} \begin{pmatrix} 1 & 0 \\ \mathcal{R}_0 & 1 \end{pmatrix} \begin{pmatrix} 1 & \tau_0 \\ 0 & 1 \end{pmatrix} \begin{pmatrix} 1 & 0 \\ \mathcal{R}_0 & 1 \end{pmatrix} \begin{pmatrix} 1 & \tau_1 \\ 0 & 1 \end{pmatrix}, \quad \mathcal{R}_0 = \frac{2\mathcal{K}_0}{\cos \varphi_0},$$

where the post-collisional state of the last reflection off the circular arc was taken as the initial point for linearization of the billiard flow along  $\gamma$ .

The stability type (elliptic, parabolic, hyperbolic) of  $\gamma$  is determined by the trace of  $M$ . In particular,  $\gamma$  is elliptic if  $-1 < \frac{1}{2} \operatorname{tr} M < 1$ . A straightforward calculation using the explicit formula (10) for  $M$  shows the following result:

**Lemma 3.1.** *The trace  $\operatorname{tr} M$  of  $M$  is given by*

$$\begin{aligned} \frac{1}{2} \operatorname{tr} M &= 1 + \frac{1}{2\tau_c} [2N - ((N-1)\tau_c - 2N\tau_1)\mathcal{R}_0] [2(2\tau_1 + \tau_0 - \tau_c) - (\tau_c - 2\tau_1)\tau_0\mathcal{R}_0] \\ &= -1 + \frac{1}{2\tau_c} [2 - (\tau_c - 2\tau_1)\mathcal{R}_0] [2(\tau_c + N(2\tau_1 + \tau_0 - \tau_c)) - ((N-1)\tau_c - 2N\tau_1)\tau_0\mathcal{R}_0]. \end{aligned}$$

In the following we are interested in finding conditions on  $\mathcal{R}_0$  such that the periodic orbit  $\gamma$  is elliptic, i.e.  $-1 < \frac{1}{2} \operatorname{tr} M < 1$  holds. For this purpose we note the following observation:

**Lemma 3.2.** *The three free paths  $\tau_0, \tau_1, \tau_c$  satisfy*

$$2\tau_1 + \tau_0 - \tau_c = \left( \frac{1}{\cos \varepsilon} - 1 \right) [2r \sin \alpha_1 - \tau_0] + 2r [\sin \alpha_1 - \sin(\alpha_1 - \varepsilon)] > 0$$

for all  $\varepsilon > 0$  (small) and all admissible  $\tau_0$ . In particular,  $2\tau_1 + \tau_0 - \tau_c = \mathcal{O}(\varepsilon)$  holds uniformly in  $\varepsilon$ .

*Proof.* By (8) and the definition of  $\tau_c$  we have

$$2\tau_1 + \tau_0 - \tau_c = \frac{2r \sin \alpha_1 - \tau_0}{\cos \varepsilon} + \tau_0 - 2r \cos \varphi_1.$$

Recall also that by (2)  $\frac{\pi}{2} - \varphi_1 = \alpha_1 - \varepsilon$ , so that  $\cos \varphi_1 = \sin(\alpha_1 - \varepsilon)$ , and therefore

$$2\tau_1 + \tau_0 - \tau_c = \frac{2r \sin \alpha_1 - \tau_0}{\cos \varepsilon} + \tau_0 - 2r \sin(\alpha_1 - \varepsilon)$$

holds, which can be readily seen to be equivalent to the claimed expression for  $2\tau_1 + \tau_0 - \tau_c$ .

Now, by the restriction (7) on the range for  $\tau_0$  it follows that the first term on the right-hand-side of the claimed expression for  $2\tau_1 + \tau_0 - \tau_c$  is positive. The second term is obviously also positive for any  $\varepsilon > 0$  (small).  $\square$

It is evident from Lemma 3.1 that  $\operatorname{tr} M$  is a quadratic function in  $\mathcal{R}_0$ . Using the factorization of  $\frac{1}{2} \operatorname{tr} M \pm 1$  derived in Lemma 3.1 we can readily obtain the solutions  $\mathcal{R}_0$  to  $\frac{1}{2} \operatorname{tr} M = \pm 1$ . In light of Lemma 3.2 we express these as follows:

$$(11) \quad \frac{1}{2} \operatorname{tr} M = 1 \iff \mathcal{R}_0 = R_1, \quad \mathcal{R}_0 = R_2$$

$$(12) \quad \frac{1}{2} \operatorname{tr} M = -1 \iff \mathcal{R}_0 = R_1 + \frac{2}{\tau_0}, \quad \mathcal{R}_0 = R_2 - \frac{2}{\tau_0}$$

where we set

$$R_1 = \frac{2}{\tau_0 - (2\tau_1 + \tau_0 - \tau_c)} - \frac{2}{\tau_0} \quad \text{and} \quad R_2 = \frac{2}{\tau_0 - \frac{1}{N}\tau_c - (2\tau_1 + \tau_0 - \tau_c)}.$$

Notice that the term in  $\frac{1}{2} \operatorname{tr} M$  that is proportional to  $\mathcal{R}_0^2$  has coefficient

$$(13) \quad \frac{N \tau_0}{2 \tau_c} [\tau_0 - (2 \tau_1 + \tau_0 - \tau_c)] \left[ \tau_0 - \frac{1}{N} \tau_c - (2 \tau_1 + \tau_0 - \tau_c) \right] = \frac{2 N \tau_0}{\tau_c} \frac{1}{R_1 + \frac{2}{\tau_0}} \frac{1}{R_2}$$

as is readily seen from Lemma 3.1. Combining (11), (12), (13) readily shows the following result:

**Proposition 3.3.** *Assume that*

$$2 \tau_1 + \tau_0 - \tau_c < \tau_0 .$$

(Recall that  $0 < 2 \tau_1 + \tau_0 - \tau_c = \mathcal{O}(\varepsilon)$  as was shown in Lemma 3.2.) Then the following hold:

(1) *The inequality*

$$0 < R_1 = \frac{2}{\tau_0} \frac{(2 \tau_1 + \tau_0 - \tau_c)}{\tau_0 - (2 \tau_1 + \tau_0 - \tau_c)} = \mathcal{O}(\varepsilon)$$

*holds. Furthermore, as  $\mathcal{R}_0$  increases from  $R_1$  to  $R_1 + \frac{2}{\tau_0}$  the trace of  $M$  decreases from 2 to  $-2$ .*

(2) *If  $\tau_0 < \frac{1}{N} \tau_c + (2 \tau_1 + \tau_0 - \tau_c)$ , i.e. if  $R_2 < 0$ , then  $\mathcal{R}_0 \mapsto \operatorname{tr} M$  is a downward pointing parabola, and as  $\mathcal{R}_0$  increases from  $R_2 - \frac{2}{\tau_0}$  to  $R_2$  the trace of  $M$  increases from  $-2$  to 2.*

(3) *If  $\frac{1}{N} \tau_c + (2 \tau_1 + \tau_0 - \tau_c) < \tau_0$ , i.e. if  $R_2 > 0$ , then  $\mathcal{R}_0 \mapsto \operatorname{tr} M$  is an upward pointing parabola, and*

$$0 < R_2 - \frac{2}{\tau_0} = \frac{2}{\tau_0} \frac{\frac{1}{N} \tau_c + (2 \tau_1 + \tau_0 - \tau_c)}{\tau_0 - \frac{1}{N} \tau_c - (2 \tau_1 + \tau_0 - \tau_c)} = \frac{2}{\tau_0} \frac{\frac{1}{N} \tau_c}{\tau_0 - \frac{1}{N} \tau_c} + \mathcal{O}(\varepsilon) ,$$

*and as  $\mathcal{R}_0$  increases from  $R_2 - \frac{2}{\tau_0}$  to  $R_2$  the trace of  $M$  increases from  $-2$  to 2.*

In order to have a geometric interpretation of the condition  $\frac{1}{N} \tau_c + (2 \tau_1 + \tau_0 - \tau_c) < \tau_0$  that is invoked in Proposition 3.3 observe that (5) combined with Lemma 3.2 shows that

$$(14) \quad \frac{1}{N} \tau_c + (2 \tau_1 + \tau_0 - \tau_c) = \frac{1}{N} \tau_c + \mathcal{O}(\varepsilon) = h + \mathcal{O}(\varepsilon) = \frac{1}{N} 2 r \sin \frac{\pi}{N} + \mathcal{O}(\varepsilon) .$$

Thus we arrive at the following observation:

**Remark 3.4.** *The geometric meaning of  $\frac{1}{N} \tau_c + (2 \tau_1 + \tau_0 - \tau_c) < \tau_0$  is that  $\tau_0$  is chosen such that it is (within an error of  $\mathcal{O}(\varepsilon)$ ) longer than the  $\frac{1}{N}$ -th part of the vertical reference orbit segment indicated by the dotted vertical red line in Fig. 5, i.e.  $\frac{1}{N} 2 r \sin \frac{\pi}{N}$ . Equivalently, it means that  $\tau_0$  is chosen longer (within  $\mathcal{O}(\varepsilon)$ ) than  $h$ .*

We conclude that Proposition 3.3 provides explicit bounds on the local geometry of  $\Gamma$ , indeed on  $\mathcal{K}_0$ , that guarantee that the periodic orbit  $\gamma$  is elliptic. Furthermore, (14) provides a clear geometric meaning of the condition distinguishing Item (2) and Item (3) in Proposition 2.

This essentially completes the proof of Item (1) of Theorem 1. What is missing still is the global construction of  $\Gamma$  so that  $\gamma$  is indeed a periodic orbit on the resulting billiard table. This will be carried out by means of specific examples for  $\Gamma$  in the next section. This will also address the additional properties that can be imposed on  $\Gamma$  as listed in Item (2) of Theorem 2, and will also establish the

nonlinear stability of  $\gamma$  and the non-vanishing of the first Birkhoff coefficient, and thereby completing the proof of Theorem 1.1.

#### 4. EXAMPLES OF BOUNDARY COMPONENTS WITH ELLIPTIC PERIODIC ORBITS

Fix  $N$ ,  $\varepsilon$ ,  $\tau_0$  and consider the periodic orbit  $\gamma$  as constructed in Section 2. Let  $\mathcal{K}_0$  denote the curvature of  $\Gamma$  at  $\Gamma_0$ . Recall (6) and note that

$$\mathcal{R}_0 = \frac{2\mathcal{K}_0}{\cos \varphi_0} = \frac{2\mathcal{K}_0}{\sin \frac{\varepsilon}{2}}$$

holds. In this section we give examples of boundary components  $\Gamma$  that have a uniformly small curvature and are such that the resulting billiard table admits an elliptic  $N + 2$ -periodic orbit, as illustrated in Fig. 5.

**4.1. Boundary components with positive curvature.** By Item (1) of Proposition 3.3, if the boundary curvature  $\mathcal{K}_0$  at  $\Gamma_0$  is such that  $R_1 < \mathcal{R}_0 < R_1 + \frac{2}{\tau_0}$ , then the periodic orbit  $\gamma$  is elliptic. In more explicit terms this condition can be written as

$$0 < \mathcal{O}(\varepsilon) = \frac{2}{\tau_0} \frac{(2\tau_1 + \tau_0 - \tau_c)}{\tau_0 - (2\tau_1 + \tau_0 - \tau_c)} < \frac{2\mathcal{K}_0}{\sin \frac{\varepsilon}{2}} < \frac{2}{\tau_0 - (2\tau_1 + \tau_0 - \tau_c)} = \frac{2}{\tau_0} + \mathcal{O}(\varepsilon).$$

Evidently the value of  $\mathcal{K}_0$  can be chosen in the above range such that  $\text{tr } M$  avoids lower order resonances, i.e.  $\text{tr } M \neq -2, -1, 0, 2$  holds. Such choice of  $\mathcal{K}_0$  clearly can be made to be uniformly  $\mathcal{O}(\varepsilon)$ .

Note, however, that the above requires that  $\mathcal{K}_0$  is positive. And since there are two such points, namely  $\Gamma_0$  and its symmetric copy, it is impossible to have a smooth  $\Gamma$  with all positive curvature. Therefore, imposing global smoothness on  $\Gamma$  requires the curvature to become negative in order for  $\Gamma$  to connect  $\Gamma_0$  and its symmetric copy.

In order for the orbit  $\gamma$  to actually exist it is necessary that the boundary component  $\Gamma$  must not intersect  $\gamma$  in places other than  $\Gamma_0$  and its symmetric copy. This can be guaranteed in many ways. On such choice of a smooth  $\Gamma$  that also stays entirely within the vertical strip of width  $\Delta$  and is symmetric about the horizontal axis is illustrated in Fig. 6 below.

If  $\Gamma$  is required only to be piece-wise smooth, then  $\Gamma$  can have positive curvature everywhere without intersecting  $\gamma$  in places other than  $\Gamma_0$  and its symmetric copy. One of the many such choices of  $\Gamma$  that also stays entirely within the vertical strip of width  $\Delta$  and is symmetric about the horizontal axis is illustrated in Fig. 7.

Regardless of the smoothness condition imposed on  $\Gamma$ , the constructions of  $\Gamma$  can be carried out for any one  $\varepsilon_0$  small enough. Then we can find a constant  $C > 0$  such that  $|\mathcal{K}|H \leq C \frac{\Delta}{H}$  holds on  $\Gamma$  for  $\varepsilon = \varepsilon_0$ . From this we construct  $\Gamma$  for all other  $\varepsilon < \varepsilon_0$  by a linear transformation that simply scales the horizontal direction by the factor  $\frac{\tan \frac{\varepsilon}{2}}{\tan \frac{\varepsilon_0}{2}}$ . This ensures that the tangent at  $\Gamma_0$  has angle  $\frac{\varepsilon}{2}$  with the vertical direction, and that the curvature  $\mathcal{K}_0$  scales proportionally to  $\varepsilon$  as well as staying within the admissible range for ellipticity of  $\gamma$ . Therefore,  $|\mathcal{K}|H \leq (1 + C) \frac{\Delta}{H}$  holds on  $\Gamma$  for all  $\varepsilon < \varepsilon_0$ , and completes the entire construction of  $\Gamma$  as claimed in Theorem 1.1, except for the nonlinear stability of  $\gamma$ .

**Remark 4.1.** *The construction of tables with elliptic orbits shown in Fig. 6 and Fig. 7 shows that hyperbolicity of moon billiards close to the folded flower billiard table (numerical evidence for this is presented in [13]) must rely on a mechanism that*

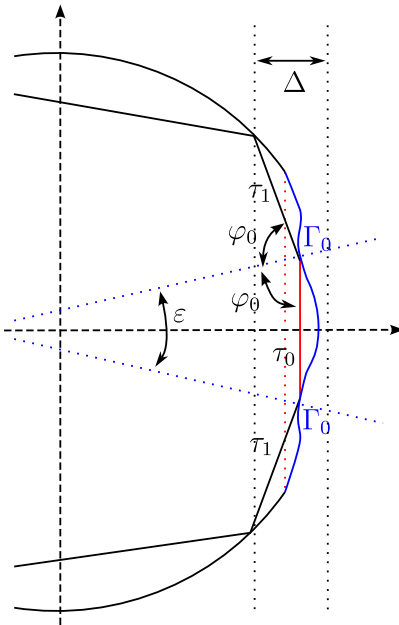


FIGURE 6. An example of a smooth symmetric boundary component  $\Gamma$  that has  $\Gamma_0 > 0$ , remains within the vertical strip of width  $\Delta$ , has curvature uniformly bounded by  $\mathcal{O}(\varepsilon)$ , and is such that the  $N + 2$ -periodic orbit  $\gamma$  is nonlinearly stable.

prevents elliptic periodic like the one shown in Fig. 7 to exist. It seems, however, unclear what exactly that mechanism is.

Using the arguments presented in [9, 11] the local geometry of boundary component  $\Gamma$  can be changed in a neighborhood of  $\Gamma_0$  by an arbitrarily small amount in the sense of the  $C^5$  topology such that the resulting  $N + 2$ -periodic orbit  $\gamma$  is nonlinearly stable in the sense that the corresponding first Birkhoff coefficient can be made non-zero. This completes the proof of Theorem 1.1 for cases of boundary components with positive curvature at  $\Gamma_0$ .

**4.2. Strictly convex boundary components.** Suppose that  $\tau_0 < \frac{1}{N} \tau_c + (2\tau_1 + \tau_0 - \tau_c)$ , i.e. suppose  $R_2 < 0$ . In more geometric terms this means (recall (14) and Remark 3.4) that  $\tau_0 < h + \mathcal{O}(\varepsilon) = \frac{1}{N} 2r \sin \frac{\pi}{N} + \mathcal{O}(\varepsilon)$ , and thus corresponds to having chosen  $\tau_0$  shorter than  $h$  (see Fig. 5).

By Item (2) of Proposition 3.3, if the boundary curvature  $\mathcal{K}_0$  at  $\Gamma_0$  is such that  $R_2 - \frac{2}{\tau_0} < \mathcal{R}_0 < R_2$ , then the periodic orbit  $\gamma$  is elliptic. In more explicit terms this condition can be written as

$$0 < \frac{2}{\frac{1}{N} \tau_c + (2\tau_1 + \tau_0 - \tau_c) - \tau_0} < -\frac{2\mathcal{K}_0}{\sin \frac{\varepsilon}{2}} < \frac{2}{\tau_0} \frac{\frac{1}{N} \tau_c + (2\tau_1 + \tau_0 - \tau_c)}{\frac{1}{N} \tau_c + (2\tau_1 + \tau_0 - \tau_c) - \tau_0}.$$

In order to better understand this condition, note that the point  $\Gamma_0$  and its symmetric copy uniquely determine a circle that contains both of them and matches the required normal lines. This circle has radius  $\rho_*$ , and thus curvature  $\mathcal{K}_* = -\frac{1}{\rho_*}$ ,

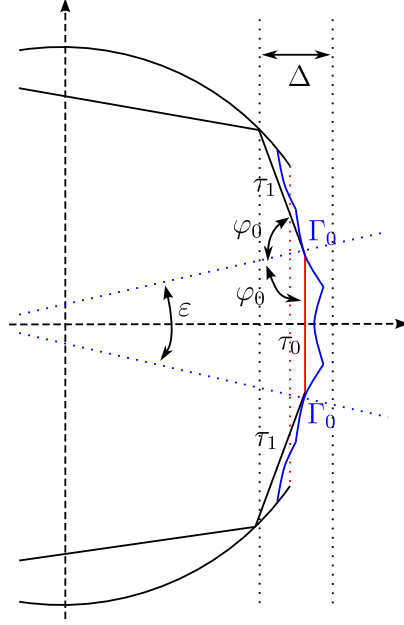


FIGURE 7. An example of a piece-wise smooth symmetric boundary component  $\Gamma$  with everywhere positive curvature that remains within the vertical strip of width  $\Delta$ , and has curvature uniformly bounded by  $\mathcal{O}(\varepsilon)$ , and is such that the  $N + 2$ -periodic orbit  $\gamma$  is nonlinearly stable.

given by

$$(15) \quad \rho_\star = \frac{\tau_0}{2 \sin \frac{\varepsilon}{2}}, \quad \mathcal{K}_\star = -\frac{2 \sin \frac{\varepsilon}{2}}{\tau_0}.$$

Because the vertical line segment of length  $\tau_0$  connects  $\Gamma_0$  and its symmetric copy and must correspond to the radial angle  $\varepsilon$  we see that  $\tau_0 = 2 \rho_\star \sin \frac{\varepsilon}{2}$  must hold.

Then the above condition on the choice of  $-\frac{2\mathcal{K}_0}{\sin \frac{\varepsilon}{2}}$  can be rewritten as

$$(16) \quad 0 < \frac{1}{2} \frac{\tau_0}{\frac{1}{N} \tau_c + (2\tau_1 + \tau_0 - \tau_c) - \tau_0} < \frac{\mathcal{K}_0}{\mathcal{K}_\star} < \frac{1}{2} \frac{\frac{1}{N} \tau_c + (2\tau_1 + \tau_0 - \tau_c)}{\frac{1}{N} \tau_c + (2\tau_1 + \tau_0 - \tau_c) - \tau_0}.$$

Note that if  $\tau_0$  is such that

$$(17) \quad \frac{1}{2} \left[ \frac{1}{N} \tau_c + (2\tau_1 + \tau_0 - \tau_c) \right] < \tau_0 < \frac{2}{3} \left[ \frac{1}{N} \tau_c + (2\tau_1 + \tau_0 - \tau_c) \right],$$

which is stronger than our earlier condition made on  $\tau_0$  at the beginning of this section, then

$$\frac{1}{2} \frac{\tau_0}{\frac{1}{N} \tau_c + (2\tau_1 + \tau_0 - \tau_c) - \tau_0} < 1 \quad \text{and} \quad 1 < \frac{1}{2} \frac{\frac{1}{N} \tau_c + (2\tau_1 + \tau_0 - \tau_c)}{\frac{1}{N} \tau_c + (2\tau_1 + \tau_0 - \tau_c) - \tau_0}$$

hold. Therefore, if (17) is satisfied, then (16) shows that the choice  $\mathcal{K}_0 = \mathcal{K}_\star$  is admissible in order to make the periodic orbit  $\gamma$  elliptic.

The geometric meaning of (17) is that  $\tau_0$  is chosen so that (within  $\mathcal{O}(\varepsilon)$ )  $\frac{1}{2} h < \tau_0 < \frac{2}{3} h$ , i.e.  $\frac{1}{N} r \sin \frac{\pi}{N} < \tau_0 < \frac{4}{3} \frac{1}{N} r \sin \frac{\pi}{N}$  holds within an error of  $\mathcal{O}(\varepsilon)$ .

Now we can construct a specific boundary component  $\Gamma$  that is convex, symmetric about the horizontal axis, and results in an elliptic  $N + 2$ -periodic orbit  $\gamma$ . For example, we can use a circular arc of curvature equal to  $\mathcal{K}_*$  that contains both  $\Gamma_0$  and its symmetric copy, and extends a little bit past them. Then the curvature is reduced symmetrically to obtain a boundary component  $\Gamma$  that does not intersect the orbit  $\gamma$  again, and remains strictly convex by keeping the curvature strictly negative. Clearly, this can be done such that  $\Gamma$  remains within the vertical strip of width  $\Delta$  (see Fig. 5). An illustration of this construction is shown in Fig. 8

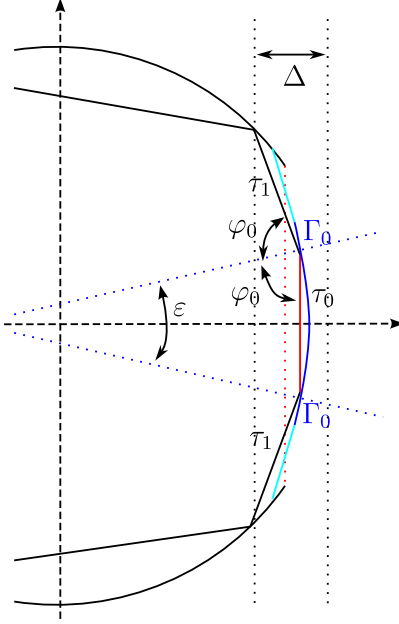


FIGURE 8. An example of a symmetric strictly convex boundary component  $\Gamma$  that remains within the vertical strip of width  $\Delta$ , has curvature uniformly bounded by  $\mathcal{O}(\varepsilon)$ , and is such that the  $N + 2$ -periodic orbit  $\gamma$  is nonlinearly stable.

further that the largest curvature (in absolute value) of  $\Gamma$  is  $|\mathcal{K}_0|$ , which we set equal to  $\mathcal{K}_*$ . Therefore, using (17) to bound  $\frac{1}{\tau_0}$ , we see that

$$\begin{aligned} \frac{|\mathcal{K}|H}{\frac{\Delta}{H}} &\leq \frac{|\mathcal{K}_*|H}{\frac{\Delta}{H}} = \frac{2 \sin \frac{\varepsilon}{2}}{\tau_0} \frac{4r \sin^2 \frac{\pi}{N}}{\sin \alpha_1 \tan \varepsilon} \leq \frac{2 \sin \frac{\varepsilon}{2}}{\frac{1}{2}[\frac{1}{N} \tau_c + (2\tau_1 + \tau_0 - \tau_c)]} \frac{4r \sin^2 \frac{\pi}{N}}{\sin \alpha_1 \tan \varepsilon} \\ &= 4N + \mathcal{O}(\varepsilon) \end{aligned}$$

holds on all of  $\Gamma$ . This shows that there exists  $C > 0$  such that for all  $\Delta > 0$  small enough  $|\mathcal{K}|H \leq C \frac{\Delta}{H}$  holds on  $\Gamma$ . It remains to prove the nonlinear stability of  $\gamma$ .

**Remark 4.2.** Note that taking  $\Gamma$  to be just a circular arc of curvature  $\mathcal{K}_*$  would not work, as this boundary component would intersect the orbit  $\gamma$  again before reaching the circular arc, and thus making the orbit  $\gamma$  not a proper billiard orbit on the resulting table. Indeed, it is this mechanism of eliminating potentially elliptic orbits that allows for hyperbolicity for lemon billiards [10, 15]

Evidently the above made choice of  $\mathcal{K}_0$  equal to  $\mathcal{K}_*$  is quite arbitrary, and can be easily adapted to other choices. As described above the resulting  $N + 2$ -periodic orbit  $\gamma$  is such that  $\text{tr} M$  avoids lower order resonances, i.e.  $\text{tr} M \neq -2, -1, 0, 2$  holds. Furthermore, using the arguments presented in [9, 11] the boundary component  $\Gamma$  as described above can be changed in a neighborhood of  $\Gamma_0$  by an arbitrarily small amount in the sense of the  $C^5$  topology such that the resulting  $N + 2$ -periodic orbit  $\gamma$  is nonlinearly stable with a non-vanishing first Birkhoff coefficient. This completes the proof of Theorem 1.1 for the case of strictly convex boundary components with everywhere strictly negative curvature.

## REFERENCES

- [1] Reginaldo Braz Batista, Mário Jorge Dias Carneiro, and Sylvie Ollifson Kamphorst, *Hyperbolicity and abundance of elliptical islands in annular billiards*, Ergodic Theory Dynam. Systems **43** (2023), no. 11, 3545–3577. MR4651576
- [2] L. A. Bunimovich, *Billiards that are close to scattering billiards*, Mat. Sb. (N.S.) **94(136)** (1974), 49–73, 159. MR342677
- [3] ———, *On ergodic properties of certain billiards*, Funkcional. Anal. i Priložen. **8** (1974), no. 3, 73–74. MR0357736 (50 #10204)
- [4] ———, *On the ergodic properties of nowhere dispersing billiards*, Comm. Math. Phys. **65** (1979), no. 3, 295–312. MR530154 (80h:58037)
- [5] ———, *Many-dimensional nowhere dispersing billiards with chaotic behavior*, Phys. D **33** (1988), no. 1-3, 58–64. Progress in chaotic dynamics. MR984610 (90m:58158)
- [6] ———, *Conditions of stochasticity of two-dimensional billiards*, Chaos **1** (1991), no. 2, 187–83 (English).
- [7] ———, *On absolutely focusing mirrors*, Ergodic theory and related topics, III (Güstrow, 1990), 1992, pp. 62–82. MR1179172 (93f:58212)
- [8] ———, *Absolute focusing and ergodicity of billiards*, Regul. Chaotic Dyn. **8** (2003), no. 1, 15–28. MR1963965 (2004a:37066)
- [9] Leonid Bunimovich and Alexander Grigo, *How smooth can convex chaotic billiard tables be?*, arXiv (2018), available at [1806.02961](https://arxiv.org/abs/1806.02961).
- [10] Leonid Bunimovich, Hong-Kun Zhang, and Pengfei Zhang, *On another edge of defocusing: hyperbolicity of asymmetric lemon billiards*, Comm. Math. Phys. **341** (2016), no. 3, 781–803. MR3452271
- [11] Leonid A. Bunimovich and Alexander Grigo, *Focusing components in typical chaotic billiards should be absolutely focusing*, Comm. Math. Phys. **293** (2010), no. 1, 127–143.
- [12] Nikolai Chernov and Roberto Markarian, *Chaotic billiards*, Mathematical Surveys and Monographs, vol. 127, American Mathematical Society, Providence, RI, 2006. MR2229799
- [13] Maria F. Correia and Hong-Kun Zhang, *Stability and ergodicity of moon billiards*, Chaos **25** (2015), no. 8, 083110, 12. MR3456006
- [14] Victor J. Donnay, *Using integrability to produce chaos: billiards with positive entropy*, Comm. Math. Phys. **141** (1991), no. 2, 225–257. MR1133266 (93c:58111)
- [15] Xin Jin and Pengfei Zhang, *Hyperbolicity of asymmetric lemon billiards*, Nonlinearity **34** (2021), no. 1, 92–117. MR4183371
- [16] Roberto Markarian, *Billiards with Pesin region of measure one*, Comm. Math. Phys. **118** (1988), no. 1, 87–97. MR954676 (89m:58122)
- [17] Ja.Ġ. SinaĠi, *Dynamical systems with elastic reflections. Ergodic properties of dispersing billiards*, Uspeli Mat. Nauk **25** (1970), no. 2(152), 141–192. MR274721
- [18] Maciej Wojtkowski, *Principles for the design of billiards with nonvanishing Lyapunov exponents*, Comm. Math. Phys. **105** (1986), no. 3, 391–414. MR848647 (87k:58165)

Email address: [alexander.grigo@ou.edu](mailto:alexander.grigo@ou.edu)

DEPARTMENT OF MATHEMATICS, UNIVERSITY OF OKLAHOMA, NORMAN OK, USA